Res Chem Intermed (2016) 42:1349–1362
DOI 10.1007/s11164-015-2089-z

Equilibrium, kinetic, and thermodynamic studies on biosorption of Cd(II) from aqueous solution by biochar

Mambo Moyo[1] · Sikwila Thokozani Lindiwe[1] · Edith Sebata[1] · Benias Chomunorwa Nyamunda[1] · Upenyu Guyo[1]

Received: 17 February 2015 / Accepted: 30 April 2015 / Published online: 20 May 2015
© Springer Science+Business Media Dordrecht 2015

Abstract The present investigation describes the use of biochar derived from an agricultural waste: the maize cob for the biosorption of Cd(II) ion. The biochar was characterized using scanning electron microscopy, surface area analysis, and Fourier transform infra-red spectroscopy. Batch experiments were performed to investigate the effects of parameters such as pH (2.0–8.0), dosage (0.2–1.2 g), contact time (5–300 min), initial metal concentration (10–100 mg L^{-1}), and temperature (20–50 °C). Kinetic data were properly fitted with the pseudo-second-order model, with the q_e (cal) value (17.21 mg g^{-1}) closer to the q_e (exp) value (18.82 mg g^{-1}). The adsorption data conforms best to the Langmuir isotherm as revealed by the lower non-linear Chi square (χ^2) value of 0.15 and a higher correlation value of 0.98 when compared to the Freundlich with a high χ^2 value of 2.65 and lower correlation value of 0.96. The maximum adsorption capacity for the biochar was 33.0 mg g^{-1}. The thermodynamic parameters ΔG^0, ΔS^0 and ΔH^0 confirmed that the biosorption was feasible, spontaneous, and endothermic. The results obtained suggest that using a low-cost biochar biosorbent for removing trace metals in contaminated water treatment plants may have great ecological and environmental significance.

Keywords Biosorption · Biochar · Cd(II) · Equilibrium · Kinetics · Thermodynamics

✉ Mambo Moyo
moyom@msu.ac.zw

[1] Department of Chemical Technology, Midlands State University, Private Bag 9055, Senga, Gweru, Zimbabwe

Introduction

Trace metal pollution has become one of the most serious environmental problems today in developing countries. The trace metals are persistent and non-biodegradable, hence their removal from the ecosystem is extremely important. Cd(II) is a trace metal that causes long-term effects such as renal dysfunction, hypertension, hepatic injury, and lung damage, and teratogenesis, and short-term effects including nausea, vomiting, diarrhoea, and cramps [1–3]. Different industrial processes, such as smelting, metal plating, and cadmium-nickel battery production are major sources of Cd(II) contamination in wastewater. The maximum recommended concentration for drinking water established by the US Environmental Protection Agency is 0.01 mg L^{-1} [4].

Pretreatment of wastewater using methods such as chemical precipitation, reverse osmosis, solvent extraction, electro dialysis, and membrane separation have substantially reduced the hazardous impact of Cd(II) on the environment, biota, and human and animal health [5–7]. However, the methods are time consuming and usually produce large amounts of sludge that can add other environmental problems [8, 9].

Several different biochar based biosorbents derived from agricultural wastes [10–13], animal wastes [14–18], and plant wastes [19–23], have been used for the removal of trace metals from aqueous solutions. In the present study, maize cobs were used as a source of biochar. Maize cobs are the maize ears without the grains. The maize cobs are inexpensive and easily available. The removal of grains from maize cobs leaves an agro-waste that has no market value and is arbitrarily discarded or burnt, which results in under-utilization of the present resource and creates pollution. Consequently, the focus of the study was to investigate the ability of maize cob-derived biochar to remove Cd(II) from aqueous solution. The biochar was characterized using scanning electron microscopy, surface area analysis, and Fourier transform infra-red spectroscopy. The effects of contact time, pH, biochar dosage, initial metal concentration, and temperature were investigated.

Materials and methods

Preparation of biosorbent

Maize cobs were collected from the Agricultural Department, Midlands State University, Gweru, Zimbabwe. The cobs were washed several times by tap water to remove all the dirt. The materials were again thoroughly washed with double distilled water. The cobs were sun dried for 24 h, and then oven dried at 100–105 °C for 24 h. The dried material was then ground and sieved to uniform size particles (150 μm). A measured amount of powdered material was fed into a lab-scale tubular reactor within a muffle furnace and pyrolysed in an N_2 atmosphere at 500–600 °C for 3 h. Then, the samples were allowed to cool down to room temperature. For activation of biochar powder, a solution of 2 M KOH (1000 mL)

was reacted with 4 g of biochar with continuous stirring, using a thermo-stirrer MSH10 for 30 min. After the reaction was completed, the biochar was placed in an oven and kept at 160 °C for 24 h. The activated biochar was collected, washed with distilled water, filtered, dried at 105 °C, and stored in sealed glass jars prior for analysis.

Characterization of the biochar

The contents of C, H, and N in the APB were analyzed using a CHN rapid elemental analyzer (Heraeus, Germany). The ash content was determined by combusting the biosorption materials at 750 °C for 5 h in open crucibles, and the oxygen content was measured based on mass difference. A Micromeritics ASAP 2020 surface area and porosity analyzer was used to measure Brunauer– Emmett–Teller (BET) surface areas of the powder. Surface morphology of biochar was examined using scanning electron microscopy (SEM, JEOL Japan), and localized elemental information on the chosen region was viewed with an energy dispersive X-ray spectroscopy (EDS, phoenix DX 60 s) in conjunction with SEM. FTIR spectroscopy (Thermo Scientific Nicolet 6700, USA) in the frequency range 450–4000 cm^{-1} was used to identify the functional groups using potassium bromide (KBr).

Biosorption experiments

A stock solution (1000 mg L^{-1}) of Cd(II) was prepared by dissolving an appropriate amount of $Cd(NO_3)_2$ from Sigma (Pretoria, South Africa) in deionized water and acidified with concentrated HNO_3 (5 mL). Batch biosorption experiments were carried out in 250 mL tightly closed conical Erlenmeyer flasks containing 50 mL of Cd(II) solution. The flasks with biosorbent dosage of 0.80 g were shaken at 20 °C at 150 rpm on a shaker for 120 min. The resultant solutions were filtered using Whatman 42 filter paper, and the supernatant liquid was analyzed using a flame atomic absorption spectrometer (Shimadzu AA-680, Japan). The percentage removal of Cd(II) was calculated using equation:

$$R = \frac{(C_o - C_e)}{C_o} \times 100\,\% \tag{1}$$

The biosorption amount (q_e) was calculated according to the following equation:

$$q_e = \frac{(C_o - C_e)V}{M} \tag{2}$$

where q_e is the amount (mg g^{-1}) of Cd(II) ions adsorbed by biochar, C_0 and C_e are the metal concentrations (mg L^{-1}) in the solution initially and after biosorption, respectively, V is the volume (L) of the solution, and m is the mass (g) of biosorbent used in the experiment. The influence of pH on the removal of Cd(II) ion was studied in the pH range 2.0–8.0. A pH meter (Crison 2001 micropH, Spain) was employed for measuring pH values in the aqueous phase after adjustment with 0.1 M NaOH or HCl from Merck (Pretoria, South Africa) were used. The ranges of

other parameters were temperature (20–50 °C), biosorbent dosage (0.2–1.2 g), contact time (5–300 min), and concentration (10–100 mg L^{-1}).

Error analysis

A test statistic such as the non-linear Chi square test (χ^2) was used to analyze the data set to confirm the best fit isotherm for the biosorption system and the calculated expression for χ^2 may be written as:

$$\chi^2 = \sum \frac{\left(q_{e,exp} - q_{e,calc}\right)^2}{q_{e,calc}} \quad (3)$$

where $q_{e,calc}$ is the calculated quantity of Cd(II) adsorbed onto biochar obtained by calculating from the various biosorption models and $q_{e,exp}$ relates to the experimental data. The value of χ^2 is smaller if data from the model are similar to the experimental data whilst the value of χ^2 will be a large number if they are different.

Results and discussion

Characterization

The elemental composition and BET characteristics of maize cob before and after pyrolysis are shown in Table 1. The measured surface area of biochar was 520 m^2 g^{-1} and is comparable to various low cost agricultural waste products such as peanut hull carbon (208 m^2 g^{-1}) [24], silk cotton hull carbon (228 m^2 g^{-1}) [25], and cassava (270 m^2 g^{-1}) [26]. The C and N content in the maize cob increased after pyrolysis due to the release of volatile components, whereas the O and H contents decreased. The total ash content was 6.75 %, showing that the biochar has a better quality and can have good biosorption capacity. The moisture content was low showing that it will not dilute the action of biochar during biosorption studies. The release of volatile components might also have caused an improvement in the specific surface area of biochar (Table 1).

Table 1 Physicochemical characteristics of the maize cob before and after pyrolysis

Physicochemical properties	Maize cob powder	Biochar
C (%)	35.25	55.62
H (%)	7.23	3.68
O (%)	32.89	18.56
N (%)	5.65	7.35
Ash content (%)	–	6.75
Moisture (%)	35.55	8.98
S_{BET} (m^2 g^{-1})	458	520

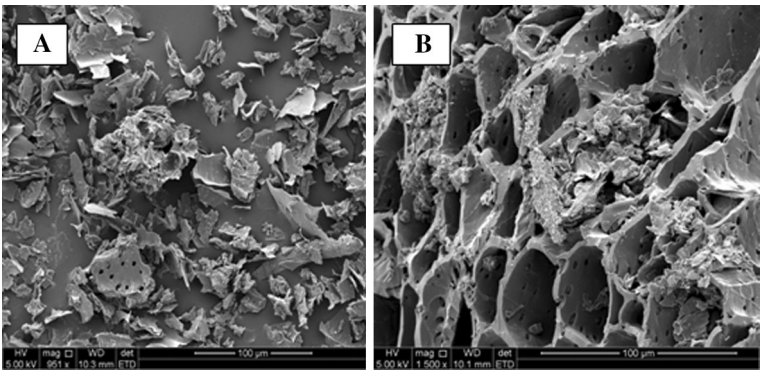


Fig. 1 SEM micrograph of biochar, **a** at magnification ×951, **b** at magnification ×1500

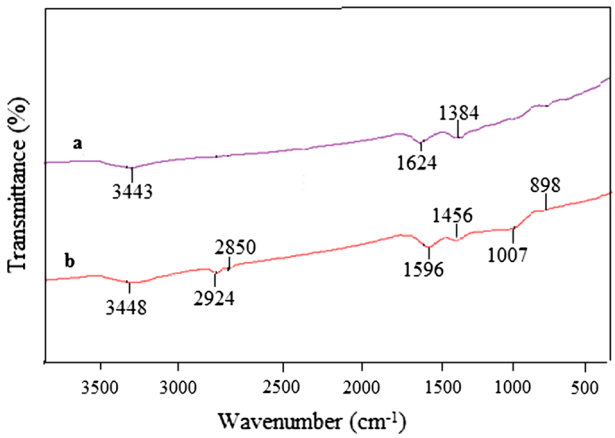


Fig. 2 FTIR spectra of biochar (*a*) before biosorption (*b*) after biosorption

Figure 1 shows the SEM micrographs of biochar at different magnifications. As observed, biochar has an irregular, rough, and porous surface that can provide binding sites for the Cd(II) ions.

FT-IR analysis was performed to investigate the functional groups in the biochar before and after Cd(II) biosorption (Fig. 2).

As shown in Fig. 2, before biosorption, the broad band at 3443 cm^{-1} is due to *v*(O–H) vibration in hydroxyl group. The bands at 2924 and 2850 cm^{-1} are assigned to –CH stretching vibration, whilst the peaks at 1624 cm^{-1} represent aromatic components (e.g., C=O stretching). The band at 1384 cm^{-1} is the characteristic of symmetrical C–O stretching vibration. The peaks observed at 1007 and 898 cm^{-1} could be due to C–O groups. After Cd(II) biosorption, some variations in the FTIR spectra were observed in Fig. 2. The peaks at 3443 cm^{-1} (–OH) and 1624 cm^{-1} (C=O) on the original biochar shifted to 3448 and 1596 cm^{-1}, respectively. The peak at 1624 cm^{-1} (aromatic components e.g., C=O) shifted to 1596 cm^{-1}. The band at 1384 cm^{-1} which represents the C–O stretching shifted to 1456 cm^{-1}.

Based on the observed changes in FTIR spectra, it can be concluded that hydroxyl and carboxylate groups might have been involved in removal of Cd(II). A schematic presentation of the biosorption process is given in Fig. 3, using the major functional groups shown in the FTIR.

Biosorption of Cd(II)

Effect of solution pH

The pH of an initial adsorbate is one of the parameters affecting biosorption through its effect on biosorbent surface charge and influencing the degree of ionization and speciation of the adsorbate [22, 27]. Hence, biosorption of Cd(II) ions by biochar was studied in the pH range of 2.0–8.0 as a function of initial pH (pH_i) and the final pH (pH_f). The results depicted in Fig. 4 shows that the effect of pH on the removal of Cd(II) ions by the biochar was less significant. The minor effect of solution pH on the biochar biosorption behavior demonstrates that the biochar has better adaptability and it may be used in different applications for treatment of environmental wastewater. A small increase in percentage removal was observed with increasing pH_i from 2.0 to 8.0. At pH 5.0, the removal percentage reached a plateau and no significance increase was noted. A maximum value of 88.2 % at pH_i of 5.0 was obtained. The surface of biochar was positive due to protonation at acidic conditions, and the Cd(II) ions could not move towards the surface of the charged biochar, hence lower removal at low pH_i. As the pH of the solution increased, the biochar were negatively charged causing some Cd(II) ions to be attracted, hence a small percentage removal was observed. Similar trends showing the effect of pH on Cd(II) removal have been reported using biochar derived from different materials [28–30].

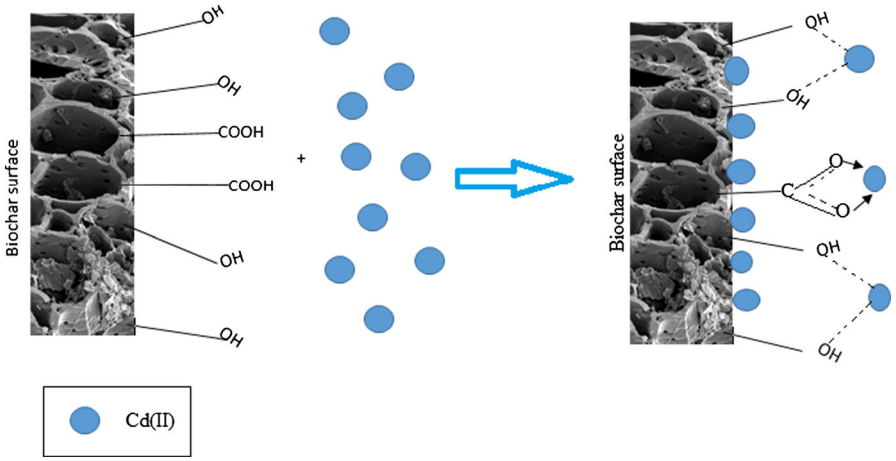


Fig. 3 Schematic illustration of proposed mechanisms for Cd(II) adsorption onto biochar

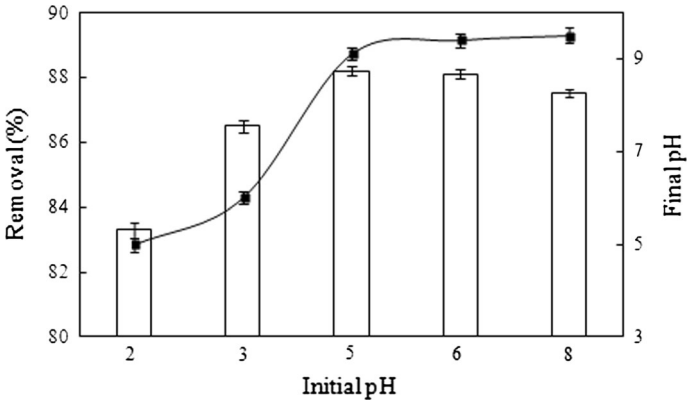


Fig. 4 Effect of pH on Cd(II) biosorption (C_0 = 10 mg L^{-1}, biochar dosage = 0.8 g, t = 120 min; *error bar* ±SD; and n = 3)

Effect of contact time

The biosorption capacity of biochar for Cd(II) was carried out and the results are shown in Fig. 5. The biosorption capacity of Cd(II) on biochar increases with rise in contact time up to 120 min, followed by slow biosorption until equilibrium is reached. The high initial biosorption rate may be attributed to more vacant surface binding sites on the surface of biochar available for biosorption during the initial stage [27]. Maximum biosorption capacity obtained at 120 min was 18.82 mg g^{-1}.

Effect of dosage

The effect of varying the biochar dosage on the uptake of Cd(II) is shown in Fig. 6. The biosorption percentage increased from 93.5 to 98.2 % with increase in biosorbent dosage from 0.2 to 0.8 g. The observed trend can be attributed to more

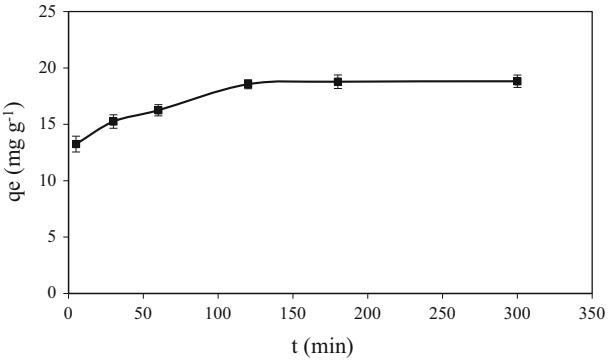


Fig. 5 Effect of contact time (dosage: 0.8 g, C_0 = 10 mg L^{-1}, pH = 5.0; *error bar* ±SD; and n = 3)

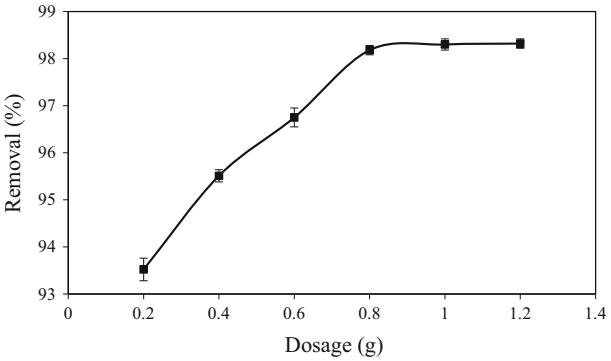


Fig. 6 Effect of dosage on biosorption of Cd (II) (pH = 5.0; t = 120 min; C_0 = 10 mg L^{-1}; *error bar* ±SD; and n = 3)

available biosorption sites as the biosorbent dosage is increased. Beyond the optimum dosage of 0.8 g, there is a notable decrease in the uptake of the Cd(II) perhaps due to overcrowding of biosorbent particles as a result of excess dosage which subsequently leads to overlapping of biomass biosorption sites.

Effect of initial metal concentration

The initial concentration of a metal ion provides an important driving force to overcome all mass transfer resistance between the aqueous and solid phases [27]. The effect of initial metal concentration on the biosorption process was analyzed within the range 10–100 mg L^{-1} (Fig. 7). As shown in Fig. 7, the biosorption uptake increased from 5.0 to 34.2 mg g^{-1}. The increase in biosorption capacity is a result of an increase in concentration gradient. Furthermore, when the initial metal ion concentration is increased, an increase in the mass transfer of Cd(II) ion between

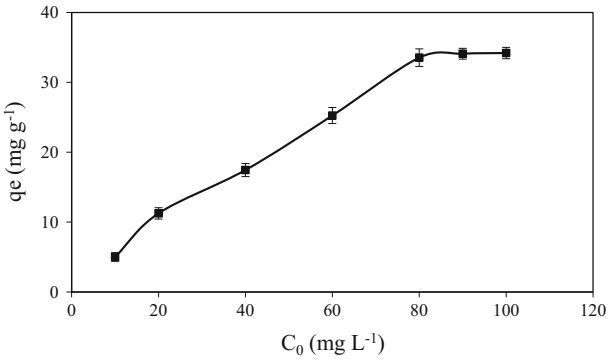


Fig. 7 Effect of initial concentration on biosorption of Cd(II) (pH = 5.0; t = 120 min; dosage = 0.8 g; *error bar* ±SD; and n = 3)

the aqueous solution and biochar powder is observed. Similar results have been reported for other biosorbents [31, 32].

Biosorption kinetics

The rate controlling steps which include mass transport, chemical reaction processes, and biosorption mechanism can be effectively investigated by different kinetic models [27]. In the present study, the pseudo-first-order and pseudo-second-order models were used for determining the mechanism of the biosorption process.

Pseudo-first-order model

The pseudo-first-order model described by the Lagergren equation is presented in linear form as [33]:

$$\log(q_e - q_t) = \log q_e - \frac{tk_1}{2.303} \tag{3}$$

where q_e and q_t are the amounts of Cd(II) adsorbed (mg g^{-1}) onto biochar at equilibrium and at time, t; k_1 (min^{-1}) is the rate constant of pseudo-first-order model and t is the time (min). The values of k_1 and q_e were calculated from the slope ($-k_1$) and intercept (log q_e) of the plot of log ($q_e - q_t$) versus t (Fig. 8a), respectively, and are presented in Table 2. The large χ^2 value and a correlation coefficient value ($R^2 = 0.89$) suggested that biosorption process does not properly follow the pseudo-first-order. This was further supported by the large difference between the calculated and experimental q_e values (Table 2).

Pseudo-second-order model

The pseudo-second-order model assumes that the rate of occupation of biosorption sites is proportional to the square of the number of unoccupied sites [34]. The linear form can be expressed as:

$$\frac{t}{q_t} = \frac{1}{q_e^2 k_2} + \frac{t}{q_e} \tag{4}$$

where k_2 is the equilibrium rate constant of pseudo-second-order model (g mg^{-1} min^{-1}). The values of q_e and k_2 are determined from the slope and intercept of the plot of (t/q_t) versus t (Fig. 8b), respectively. The high correlation coefficient value ($R^2 = 0.99$), low χ^2 value and a good agreement between calculated and experimental q_e value (Table 2) indicated the applicability of the pseudo-second-order kinetic model for biochar-Cd (II) systems.

Biosorption isotherms

Isotherms are useful in designing biosorption process systems since equilibrium studies determine the biosorption capacities of the biosorbents. In order to come up

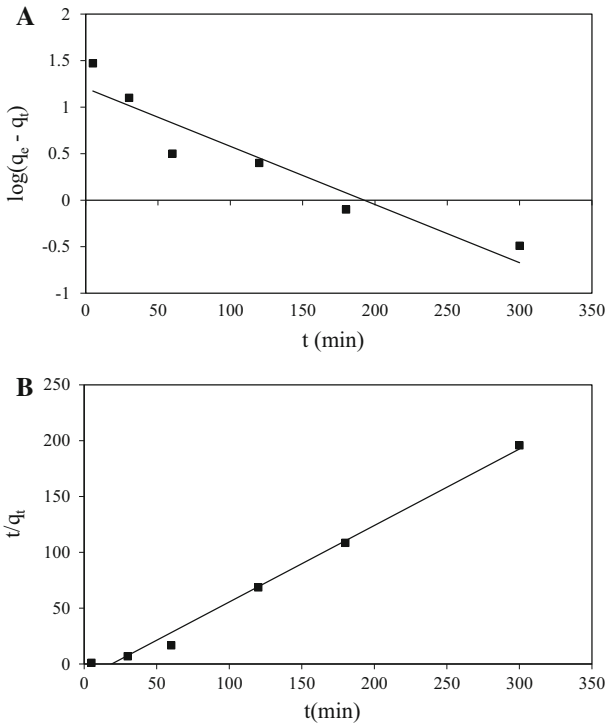


Fig. 8 **a** Pseudo-first-order, **b** pseudo-second-order plots for Cd(II) biosorption (pH = 5.0; C_0 = 10 mg L^{-1}; dosage = 0.8 g; *error bar* ±SD; and n = 3)

Table 2 Rate constants for Cd(II) biosorption on biochar

Experimental value q_e (mg g^{-1})	Pseudo-first-order				Pseudo-second-order			
	q_e (mg g^{-1})	k_1 (min^{-1})	R^2	χ^2	q_e (mg g^{-1})	k^2 (g mg^{-1} min^{-1})	R^2	χ^2
18.82	3.34	0.0145	0.89	5.25	17.21	0.0036	0.99	0.25

with an optimum design for successful biosorptive removal of Cd(II) from wastewater, it is vital to establish the best correlation for the equilibrium isotherms. The two-parameter isotherm models, Langmuir [35] and Freundlich [36], were used to interpret the experimental data (Fig. 9a, b).

A linear plot was obtained after plotting $1/q_e$ versus 1/Ce with a high correlation coefficient value and smaller χ^2 value (Table 3). It can be concluded that biosorption follows the Langmuir model of biosorption. The suitability of the Langmuir isotherm can further be tested using a dimensionless constant known as the separation factor (R_L). The constant is expressed in form of an equation:

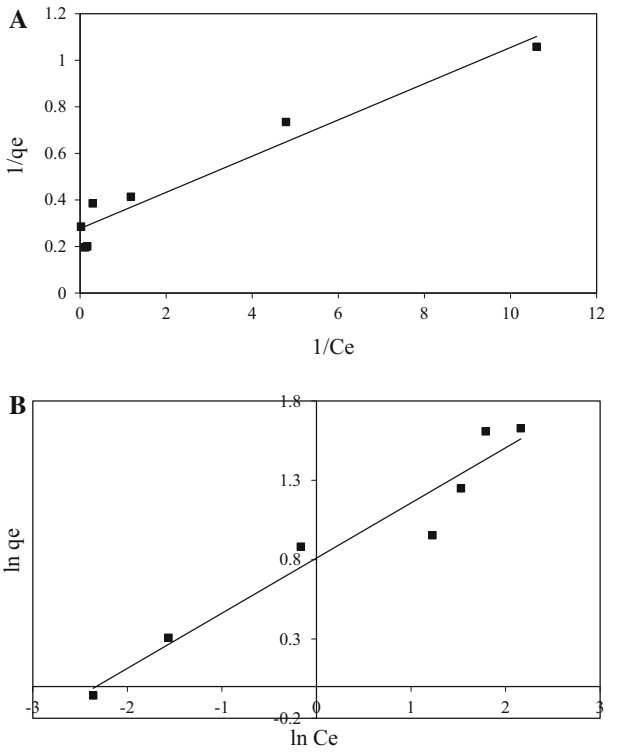


Fig. 9 **a** Langmuir isotherm, **b** Freundlich isotherm for Cd(II) biosorption

Table 3 Isotherm model parameters for Cd(II) biosorption onto biochar

Isotherm model	Parameters	Value
Langmuir	q_{max} (mg g^{-1})	33.0
$\frac{1}{q_e} = \frac{1}{q_{max}} + \left(\frac{1}{bq_{max}}\right)\frac{1}{C_e}$	b (L mg^{-1})	0.037
	R^2	0.98
	χ^2	0.15
Freundlich	K_F (mg g^{-1})	2.25
$\ln q_e = \ln K_F + \frac{1}{n}\ln C_e$	n	2.14
	R^2	0.96
	χ^2	2.65

$$R_L = \frac{1}{1 + bC_m} \tag{5}$$

where C_m is the initial Cd(II) concentration (10 mg L^{-1}). The value of R_L indicates the type of the isotherm to be either unfavorable when $R_L > 1$, linear if $R_L = 1$, and favorable if $0 < R_L < 1$ or $R_L = 0$. The calculated R_L value is 0.73 indicating that the biosorption of Cd(II) is favorable.

From the Freundlich equation, a plot of ln q_e versus ln C_e (Fig. 9b) gives a straight line, and K_F and n can be calculated from the intercept and slope, respectively. The calculated value of Freundlich constant n was 2.14 (Table 3) and represented beneficial biosorption since it falls between 1 and 10. However, the high χ^2 value of 2.65 and lower correlation value of 0.96 showed that biosorption was not very favorable as compared to the Langmuir isotherm.

Comparison of biochar with other biosorbents

The comparison of the maximum biosorption capacities of various biosorbents including biochar is summarized in Table 4. The biosorption capacity of biochar was found to be comparable and moderately higher than those of many corresponding biosorbents in the literature [13, 20, 22, 28, 37]. Animal derived biochar such as cow manure and pig manure biochar have higher biosorption capacity than maize cob derived biochar. However, the easy availability and cost effectiveness of maize cob biochar are additional advantages, making it a better biosorbent for treatment of Cd(II) wastewater.

Biosorption thermodynamics

In the present study, the aqueous solution temperature was varied from 20 to 50 °C, keeping all other parameters constant. The removal capacity increased with increasing temperature from 20 to 50 °C. Thermodynamic parameters such as standard Gibbs free-energy change (ΔG^0), the entropy change (ΔS^0) and the enthalpy change (ΔH^0) were estimated using Eqs. (6–8):

$$K_d = \frac{q_e}{C_e} \tag{6}$$

$$\ln K_d = \frac{\Delta S^o}{R} + \frac{\Delta H^o}{RT} \tag{7}$$

Table 4 Comparison of maximum biosorption capacity of biochar with other biosorbents

Biosorbent	q_{max} (mg g^{-1})	Reference
Rice straw biochar	34.13	[13]
Dairy manure biochar	51.4	[15]
Oak bark char	5.40	[20]
Pine bark char	0.34	
Oak wood char	0.37	
Switchgrass biochar	34.0	[22]
Cassava stem biochar	24.88	[28]
Cow manure biochar	114.75; 118.40	[29]
Oil shale ash	12.05	[37]
Buffalo weed biochar	11.63	[38]
Maize biochar	33.0	Present study

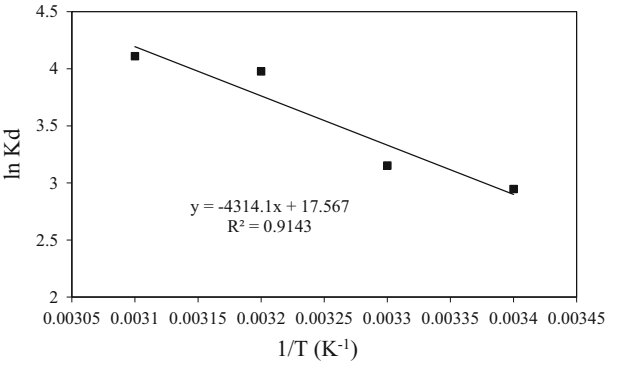


Fig. 10 van 't Hoff plot for the biosorption of Cd(II) onto the biochar (pH = 5.0; t = 120 min; C_0 = 10 mg L^{-1}; dosage = 0.8 g)

$$\Delta G^o = \Delta H^o - T\Delta S^o \tag{8}$$

where, R is the ideal gas constant (8.314 $Jmol^{-1}$ K^{-1}), T is the temperature, and K_d is the thermodynamic equilibrium constant. The intercept and slope of the van 't Hoff plot of ln K_d versus $1/T$ (Fig. 10) were used to determine the ΔS^0 and ΔH^o values. The ΔH^0 parameter was calculated to be +35.87 kJ mol^{-1}, showing an endothermic biosorption processes. The ΔS^0 parameter was found to be +0.15 kJ mol^{-1} K^{-1} for Cd(II) biosorption. The positive ΔS^0 reflects the formation of a chaotic solid/solution interface as the Cd(II) interact with the functional groups on the biochar, leading to structural changes The Gibbs free energy change (ΔG^0) was calculated to be −6.91, −8.37, −6.84, −9.83, and −11.29 kJ mol^{-1} at 20, 30, 40, and 50 °C, respectively. The negative ΔG^0 values indicated the feasibility and spontaneous nature of the biosorption. The temperature-dependent increment of negativity for ΔG^0 indicates that the biosorption process is favored at higher temperature.

Conclusions

In the present study, the use of biochar as a biosorbent was investigated for removing of Cd(II) ions from aqueous solution. Cd(II) biosorption onto the biochar was not strongly influenced by the solution pH. The adsorption capacity of biochar was determined as 33.0 mg g^{-1}. FTIR spectroscopic analysis of metal-loaded biomass sample confirmed the result. The kinetic studies revealed that the biosorption process followed the pseudo-second-order kinetic model well. The calculated thermodynamic parameters showed the that the biosorption of Cd(II) ions onto biochar is feasible, spontaneous, and endothermic.

Acknowledgments The authors are grateful for the Department of Chemical Technology, Midlands State University, Gweru, Zimbabwe, for providing facilities.

References

1. T.G. Kazi, N. Jalbani, N. Kazi, M.K. Jamali, M.B. Arain, H.I. Afridi, A. Kandhro, Z. Pirzado, Ren. Fail. **30**(7), 737–745 (2008)
2. E. Kalkan, H. Nadaroglu, N. Dikbaş, E. Taşgin, N. Çelebi, Pol. J. Environ. Stud. **22**(2), 417–429 (2013)
3. R.A. Anayurt, A. Sari, M. Tuzen, Chem. Eng. J. **151**, 255–261 (2009)
4. B. Volesky, *Biosorption of Heavy Metals* (CRC Press, USA, 1990), p. 14
5. M.S. Al-Masri, Y. Amin, B. Al-Akel, T. Al-Naama, Appl. Biochem. Biotechnol. **160**, 976–987 (2010)
6. P.S. Kumar, S. Ramalingam, V. Sathyaselvabala, S. Dinesh Kirupha, S. Sivanesan, Desalination **266**, 63–71 (2011)
7. M. Moyo, G. Nyamhere, E. Sebata, U. Guyo, Desalin. Water Treat. 1–11 (2014). doi: 10.1080/19443994.2014.968217
8. T.A. Saleh, V.K. Gupta, Environ. Sci. Pollut. Res. **19**, 1224–1228 (2012)
9. H. Daraei, A. Mittal, J. Mittal, H. Kamali, Desalin. Water Treat. **52**(7–9), 1307–1315 (2014)
10. Y. Chun, G.Y. Sheng, C.T. Chiou, B.S. Xing, Environ. Sci. Technol. **38**(17), 4649–4655 (2004)
11. B.L. Chen, Z.M. Chen, Chemosphere **76**, 127–133 (2009)
12. Z.G. Liu, F.S. Zhang, J. Hazard. Mater. **167**, 933–939 (2009)
13. X. Han, C. Liang, T. Li, K. Wang, H. Huang, X. Yang, Biomed. Biotechnol. **14**(7), 640–649 (2013)
14. J. Meng, X. Feng, Z. Dai, X. Liu, J. Wu, J. Xu, Environ. Sci. Pollut. Res. **21**, 7035–7046 (2014)
15. X.Y. Xu, X.D. Cao, L. Zhao, H.L. Wang, H.R. Yu, B. Gao, Environ. Sci. Pollut. Res. **20**, 358–368 (2013)
16. X.D. Cao, L.N. Ma, B. Gao, W. Harris, Environ. Sci. Technol. **43**, 3285–3291 (2009)
17. M. Uchimiya, I.M. Lima, K.T. Klasson, S.C. Chang, L.H. Wartelle, J.E. Rodger, J. Agric. Food Chem. **58**, 5538–5544 (2010)
18. M.X. Guo, G.N. Qiu, W.P. Song, Waste Manag. **30**, 308–315 (2010)
19. L.C. Bornemann, R.S. Kookana, G. Welp, Chemosphere **67**(5), 1033–1042 (2007)
20. D. Mohan, C.U. Pittman, M. Bricka, F. Smith, B. Yancey, J. Mohammad, P.H. Steele, M.F. Alexandre-Franco, V. Gomez-Serrano, H. Gong, J. Colloid Interface Sci. **310**, 57–73 (2007)
21. B.L. Chen, D.D. Zhou, L.Z. Zhu, Environ. Sci. Technol. **42**(14), 5137–5143 (2008)
22. P. Regmi, G.L.J. Moscoso, S. Kumar, X. Cao, J. Mao, G. Schafran, J. Environ. Manag. **109**, 61–69 (2012)
23. M. Li, Q. Liu, L. Guo, Y. Zhang, Z. Lou, Y. Wang, G. Qian, Bioresour. Technol. **141**, 83–88 (2013)
24. K. Periasamy, C. Namasivayam, Chemosphere **32**(4), 769–789 (1996)
25. K.S. Thangamani, M. Sathishkumar, Y. Sameena, N. Vennilamanii, K. Kadirvelu, S. Pattabi, S.E. Yun, Bioresour. Technol. **98**, 1265–1269 (2007)
26. S. Rajeshwarisivaraj, P. Sivakumar, V. Senthilkumar, Bioresour. Technol. **80**, 233–235 (2001)
27. M. Moyo, U. Guyo, G. Mawenyiyo, N.P. Zinyama, B.C. Nyamunda, J. Ind. Eng. Chem., xxx, xxx–xxx, *in press.* (2015) doi:10.1016/j.jiec.2014.12.026
28. S. Prapagdee, S. Piyatiratitivorakul, A. Petsom, Environ. Asia **7**(2), 60–69 (2014)
29. D. Kołodyńska, R. Wnętrzak, J.J. Leahy, M.H.B. Hayes, W. Kwapiński, Z. Hubicki, Chem. Eng. J. **197**, 295–305 (2012)
30. Y. Yang, Z. Wei, X. Zhang, X. Chen, D. Yue, Q. Yin, L. Xiao, L. Yang, Bioresour. Technol. **171**, 227–232 (2014)
31. U. Guyo, J. Mhonyera, M. Moyo, Process Saf. Environ. Prot. **93**, 192–200 (2015)
32. A.K. Sheku, M. Moyo, C.M. Zvinowanda, O.J. Okonkwo, Desalin. Water Treat. 1–9 (2015). doi: 10.1080/19443994.2015.1004116
33. P.R. Sheha, J. Colloid Interface Sci. **310**, 18–26 (2007)
34. S.R. Shukla, R.S. Pai, Bioresour. Technol. **96**, 1430–1438 (2005)
35. I. Langmuir, J. Am. Chem. Soc. **38**(2), 2221–2295 (1916)
36. H.M.F. Freundlich, J. Phys. Chem. **57**, 384–470 (1906)
37. B. Zhu, Z. Xiu, N. Liu, H. Bi, C. Lv, Oil Shale **29**(3), 268–278 (2012)
38. K. Yakkala, M.R. Yu, H. Roh, J.K. Yang, Y.Y. Chang, Desalin. Water Treat. **51**, 7732–7745 (2013)